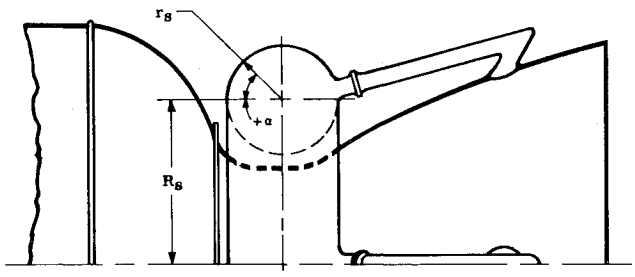

Fig. 3 Secondary storage torus configuration.

where

$$\xi \equiv L_s/2R_s \tag{6}$$

$$\beta \equiv \rho_p\sigma_s\eta_s P_p/\rho_s\sigma_p\eta_p P_s \tag{7}$$

Taking the limit of Eq. (5) as $\xi \to 0$ and $\xi \to \infty$ we have

$$1.33 \geqq \Delta W_p/W_s \geqq 1 \quad \text{for} \quad \beta = 1$$

For the torus configuration (Fig. 3) the stresses developed are[1]

$$\sigma_h = \frac{P_s r_s}{2t} \qquad \sigma_m = \frac{P_s r_s(2R_s + r_s\sin\alpha)}{2t(R_s + r_s\sin\alpha)} \tag{8}$$

but

$$(\sigma_m)_{\max} = Pr_s(2R_s - r_s)/2t(R_s - r_s) \tag{9}$$

and since $\sigma_h < (\sigma_m)_{\max}$, the minimum allowable wall thickness is

$$(t_{\min})_{\text{all}} = Pr_s(2R_s - r_s)/2(\sigma_m)_{\max}(R_s - r_s) \tag{10}$$

Therefore the secondary storage weight is given by

$$W_s = \frac{2\pi^2 r_s^2 R_s\rho_s P_s}{\sigma_s}\left[\frac{2R_s - r_s}{R_s - r_s}\right] \tag{11}$$

By equating storage volumes

$$\Delta L_p = 2\pi R_s(\eta_s/\eta_p)(r_s/R_p)^2 \tag{12}$$

the tradeoff becomes.

$$\Delta W_p/W_s = \beta(\xi - 1)/(\xi - \tfrac{1}{2}) \tag{13}$$

where $\xi \equiv R_s/r_s$ and β is given by Eq (7). Taking limits for $\xi \to 1$ and $\xi \to \infty$ for $\beta = 1$,

$$1 \geqq \Delta W_p/W_s \geqq 0$$

Conclusions

Figure 4 shows that, for $\beta \geqq 1$ and small ξ, a substantial weight saving may be realized by using the cylindrical-hemispherical secondary storage configuration as opposed to added primary storage; a maximum value for $\Delta W_p/W_s$ occurs at $\xi = 0$, which reduces to a spherical configuration. On the other hand, the torus configuration will impose a considerable weight penalty unless $\beta \gg 1$ can be obtained along with relatively large radius ratios.

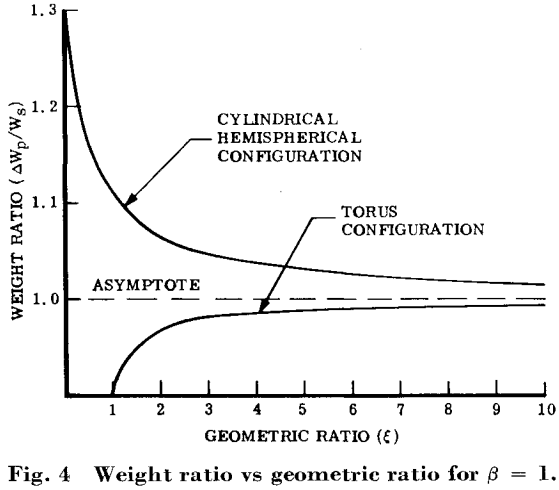

Fig. 4 Weight ratio vs geometric ratio for $\beta = 1$.

A family of curves like those presented in Fig. 4 can be generated for various values of β, all of which have asymptotic values equal to β. The preceding conclusions have been made assuming that the weights of the supporting hardware associated with secondary storage are small as compared with the weight of the secondary pressure vessel itself.

Reference

[1] Koelle, H. H., *Handbook of Astronautical Engineering* (McGraw-Hill Book Co., Inc., New York, 1961), pp. 22–71, 22–72.

Cavitation Damage Resistance of Materials in Liquid Sodium

A. Thiruvengadam,* C. Couchman III,* and H. S. Preiser*
Hydronautics, Inc., Laurel, Md.

Nomenclature

S_e = strain energy
Y = yield strength
T = ultimate tensile strength
ϵ = ultimate tensile elongation
I = intensity of cavitation damage
i = average depth of erosion
t = test duration

RESEARCH on cavitation damage in liquid alkali metals at high temperatures is motivated by the need for development of lightweight auxiliary power generating equipment for future space vehicles in which liquid alkali metals are to be used as the thermodynamic working fluid. Systematic investigations have been started to study the cavitation damage resistance of metals in liquid sodium.

The experimental facility used for these investigations has been described in detail along with an improved version of this design in Ref. 1. In essence, a simple unpressurized purge

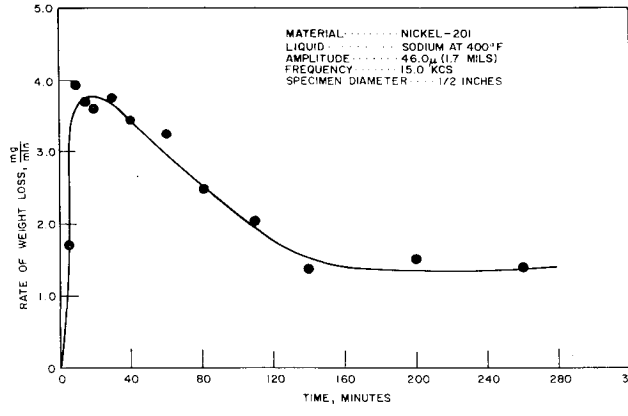

Fig. 1 Effect of time on rate of weight loss of 201 nickel.

Presented as Preprint 64-363 at the 1st AIAA Annual Meeting, Washington, D. C., June 29–July 2, 1964; revision received September 14, 1964. These investigations were supported by NASA, under Contract No. NASr-105.

* Research Scientist.

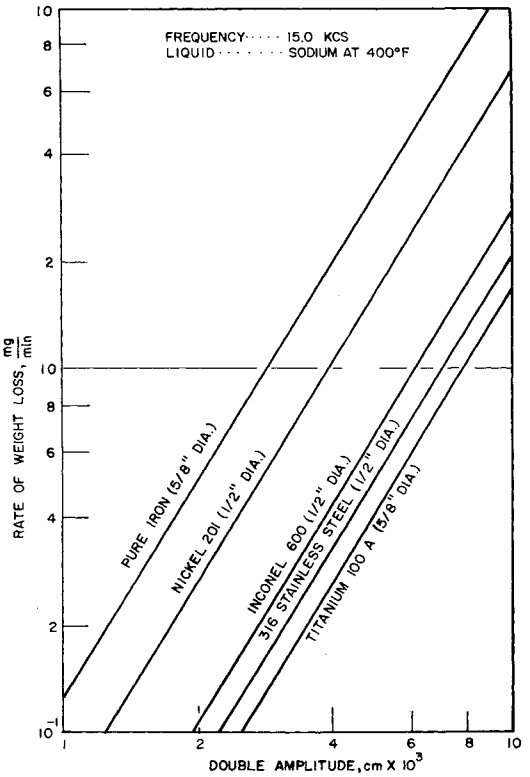

Fig. 2 Effect of displacement amplitude on the rate of weight loss in the steady-state zone.

type of dry box was used in which air was removed from the enclosure by displacement with industrial grade argon as the cover gas. Regular grade dry sodium was used in these tests. A magnetostriction transducer was used to vibrate the test specimen in the liquid.

It has been the general practice in the past to test all materials over an arbitrarily selected constant duration and to compare the cumulative weight loss as an indication of the cavitation damage resistance. Recent investigations using distilled water at 80°F have pointed out that this is not a good practice, since the rate of damage is dependent on the test duration itself.[2,3] This result has been confirmed for the case of liquid sodium at 400°F using five metals (pure iron, 201 nickel, 316 stainless steel, 600 inconel, 100A titanium). The typical data for one metal, nickel, is shown in Fig. 1. The data for other metals are given in Ref. 6. An analysis of these data reveals that the relationship between

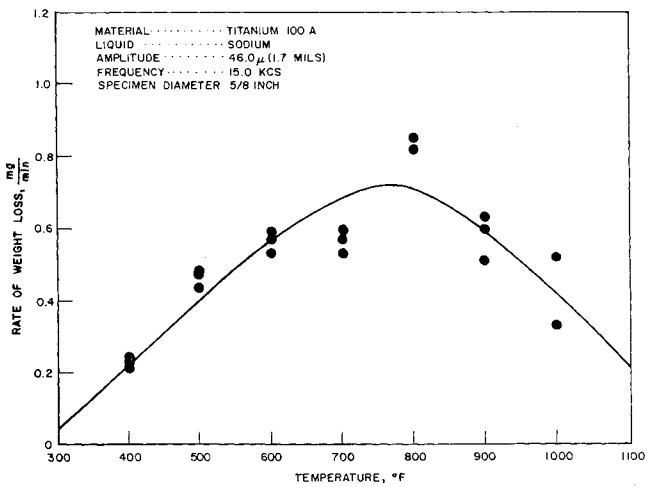

Fig. 3 Effect of sodium temperature on rate of weight loss.

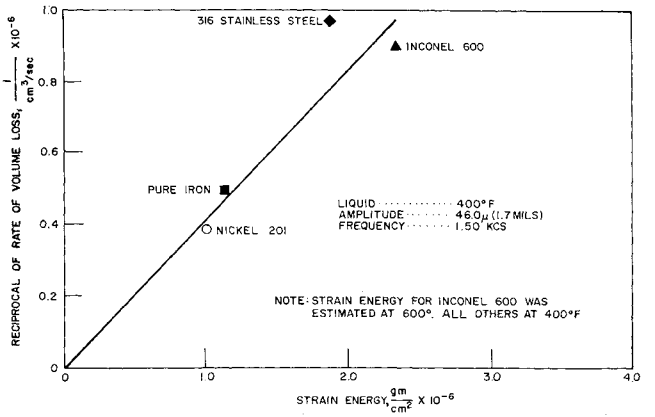

Fig. 4 Relationship between the estimated strain energy and the reciprocal of the rate of volume loss.

the rate of cavitation damage and the test duration can be divided into four zones as follows: 1) incubation zone, 2) accumulation zone, 3) attenuation zone, and 4) steady-state zone. The incubation zone is not apparent in Fig. 1 since the initial test durations were not short enough to detect it. It is important to understand the interacting influence of testing time before any attempt is made to compare the cavitation damage resistance of different materials.

It has also been confirmed that the cavitation damage rate varies as the square of the displacement amplitude of the specimen in the steady-state zone for liquid sodium at 400°F (Fig. 2). The effect of temperature up to 1000°F in the steady-state zone is shown in Fig. 3 for 100A titanium.

There have been many attempts in the past to correlate the mechanical properties of the metal with cavitation damage. Recent efforts to correlate the strain energy of the metal (area of the stress strain diagram from a simple tensile test) have offered the best promise.[4,5] Similar correlation is shown in Fig. 4. In this case, the estimated strain energy as given by the following equation

$$S_e = (Y + T)\epsilon/2 \tag{1}$$

was used since complete stress-strain curves at these temperatures for the metals tested are a rarity. Considering the fact that the values of mechanical properties used for the analysis are only typical values and that they may vary from heat to heat, the correlation between the estimated strain energy and the cavitation damage resistance is good.

A reasonably successful formulation of the concept of absolute intensity of cavitation damage has been accomplished recently.[2] The intensity is defined as the power absorbed by unit area of the material and is given by

$$I = iS_e/t \tag{2}$$

The value of I was calculated for the present case in the steady-state zone to be 2.3×10^{-4} w/cm² as compared to an estimated value of 1.5×10^{-4} w/cm² in distilled water at 80°F for a double amplitude of 1.5×10^{-3} in. and a frequency of 15 kc. Hence the intensity of cavitation damage in liquid sodium at 400°F is about one and one half times that in distilled water at 80°F.

References

[1] Preiser, H. S., Thiruvengadam, A., and Couchman, C., III, "Cavitation damage research facilities for high temperature liquid alkali metal studies," Symposium on Cavitation Research Facilities and Techniques, ASME, Fluids Engineering Conference (May 1964).

[2] Thiruvengadam, A., "A comparative evaluation of cavitation damage test devices," Symposium on Cavitation Research Facilities and Techniques, ASME, Fluids Engineering Conference (May 1964).

[3] Thiruvengadam, A. and Preiser, H. S., "On testing materials for cavitation damage resistance," Hydronautics, Inc., TR233-3 (1964).

[4] Thiruvengadam, A., "A unified theory of cavitation damage," J. Basic Eng. **85**, 365–376 (September 1963).

[5] Thiruvengadam, A. and Waring, S., "Mechanical properties of metals and their cavitation damage resistance," Hydronautics, Inc., TR233-5 (August 1964).

[6] Thiruvengadam, A. Couchman, C., III, and Preiser, H. S., "Cavitation damage resistance of materials in liquid sodium," AIAA Preprint 64-363 (June 29–July 2, 1964).

Large Post-Saturn Launch Vehicles: Why? When? What?

WILLIAM G. HUBER*
NASA Marshall Space Flight Center, Huntsville, Ala.

LAUNCH vehicles continue to be one of the major pacing items in the progress of space exploration. The largest launch vehicle now under development is the Saturn V; however, planning is underway for a post-Saturn vehicle that could greatly increase our capabilities for planetary exploration. This planning effort must first determine under what conditions a post-Saturn is justified. In other words, what is the size of space programs beyond which it is desirable to develop a launch vehicle larger than Saturn V? Then by having some indication of the future program, the questions of why we need a post-Saturn, when we need it, and what is the best concept can be answered.

Possible Vehicle Concepts

In order to proceed with the missions analysis work in parallel with the vehicle design effort, representative or baseline configurations were selected in each vehicle class (Fig. 1).† The selection of these baselines does not mean that they are best in their class, but only representative of the technology and availability offered by the class. It is then possible to make certain interclass comparisons with these baseline concepts.

Class I comprises expendable vehicles with propulsion systems currently under development. These include the M-1, the large solid, and the F-1 or an up-rated version of the F-1. The first-stage diameter is 65.5 ft; the second-stage diameter is 60 ft; and both stages use separate propellant tanks.

Class II represents advanced technology, principally in propulsion and recovery. New propulsion systems may use high chamber pressure, up to 3000 psia, and unconventional nozzles achieving some degree of altitude compensation. These advanced propulsion concepts are expected to improve the cost effectiveness of class II by 15%. The most desirable propulsion system is yet to be determined, since a great deal of experimental work is needed to verify the performance assumptions. Recovery and reuse of the first stage offers a 40% improvement in cost effectiveness for a launch rate of about 10/yr. Recovery of the second stage can offer further improvement of about 8%; however, the technical problems associated with recovery of items of this size from near-orbital velocities are serious, and at this time are not considered worth the potential gains for the class II.

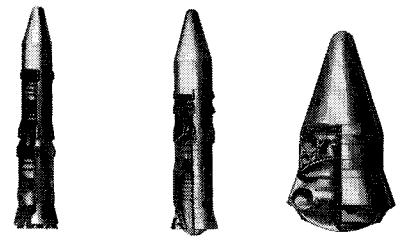

CLASS	I	II	III	
HEIGHT (FT)	460	420	210	
			1 STAGE	2 STAGE
ENGINES	18 F-1A/3M-1	18/2 @ 1000K	18 @ 1000K	18/3 @ 1000K
THRUST (M-LB)	32.4	18	18	18
LAUNCH WT. (M-LB)	25.2	14.4	12-14.4	14.4
PAYLOAD (K-LB)	980	942	460-826	1250
PROP. MASS FRACTION	.920/.904	.897/.883	.928	.928/.922
GROSS WT./PAYLOAD	25.7	15.3	14.5	11.3

Fig. 1 Baseline post-Saturn vehicles.

Class III concepts utilize very advanced technology in the areas of propulsion, structures, and recovery from near orbital velocity. The ideal class III concept is a single-stage-to-orbit, fully recoverable vehicle. Several configurations have been studied. Analyses have shown the vehicle performance to be extremely sensitive to specific impulse and dry stage weight assumptions. Special features may include expendable tanks, solid and liquid JATO units, fluorine substitution, expendable second stages, and variable payload capability. A representative class III configuration was selected and is shown in Fig. 1. This is a basic single-stage-to-orbit, fully recoverable concept with 826,000-lb payload capability. For larger payload missions, an expendable second stage could give a 1,250,000-lb payload capability. The vehicle is about 120 ft in diameter and 220 ft high with second stage and payload.

Mission Analysis

In order to attempt to determine the role of a post-Saturn vehicle, four different mission models were developed, as indicated in Table 1. The missions assumed covered the orbital, lunar, and both the manned and unmanned planetary categories, and were constructed to represent possible follow-ons to existing programs for the 1970 to 1990 period. Table 1 indicates the magnitudes of the small and large programs without going into detail. Besides varying the number of missions, the size of each mission was varied in the manned planetary area. As an example, the initial manned Mars landing was assumed to be with a fleet of four ships for the large programs and only two ships for the small programs. Shown in Fig. 2 is the effect of schedule on the programs. For simplicity, the two extremes are shown. There is some variation of the selected missions with schedule. For example, a Mars capture mission was assumed for the small programs, but not for the large ones. For the small programs, the most ambitious mission selected was a manned Mars landing. Both the large programs included a Mars synodic base, and for the one on an optimistic schedule, another even more advanced mission was assumed.

Table 1 Assumed mission objectives

Program schedule	No. of orbital manned stations	Lunar base size[a]	No. of planetary missions: Unmanned	No. of planetary missions: Manned
Large O[b]	24	80	37	11
Large P[b]	24	80	37	7
Small O	10	12	18	8
Small P	10	12	18	5

[a] Number of men.
[b] O = optmistic schedule, P = pessimistic schedule (see Fig. 2).

Presented as Preprint 64-279 at the 1st AIAA Annual Meeting, Washington, D. C., June 29–July 2, 1964; revision received August 28, 1964.

* Special Assistant to the Director, Future Projects Office. Member AIAA.

† A fourth class, not discussed herein, would comprise a chemical class I or II first stage with a nuclear second stage.